

Dual-functional c(RGDyK)-decorated Pluronic micelles designed for antiangiogenesis and the treatment of drug-resistant tumor

Yanzuo Chen^{1,2}Wei Zhang^{2,3}Yukun Huang¹Feng Gao¹Xiaoling Fang²

¹Department of Pharmaceutics, School of Pharmacy, East China University of Science and Technology, ²Key Laboratory of Smart Drug Delivery, Ministry of Education and PLA, School of Pharmacy, Fudan University, Shanghai, People's Republic of China; ³CONRAD, Department of Obstetrics and Gynecology, Eastern Virginia Medical School, Arlington, VA, USA

Abstract: Dual-functional drug delivery system was developed by decorating c(RGDyK) (cyclic RGD [arginine-glycine-aspartic acid] peptide) with Pluronic polymeric micelles (c[RGDyK]-FP-DP) to overcome the drawbacks of low transport of chemotherapeutics across the blood-tumor barrier and poor multidrug-resistant (MDR) tumor therapy. c(RGDyK) that can bind to the integrin protein richly expressed at the site of tumor vascular endothelial cells and tumor cells with high affinity and specificity was conjugated to the *N*-hydroxysuccinimide-activated PEO terminus of the Pluronic F127 block copolymer. In this study, decreased tumor angiogenic and increased apoptotic activity in MDR cancer cells were observed after the treatment with c(RGDyK)-FP-DP. c(RGDyK)-FP-DP was fully characterized in terms of morphology, particle size, zeta potential, and drug release. Importantly, *in vitro* antiangiogenesis results demonstrated that c(RGDyK)-FP-DP had a significant inhibition effect on the tubular formation of human umbilical vein endothelial cells and promoted cellular apoptotic activity in MDR KBv cells. In addition, the growth inhibition efficacy of KBv tumor spheroids after crossing the blood-tumor barrier was obviously increased by c(RGDyK)-FP-DP compared to other control groups. Results suggested that c(RGDyK)-decorated Pluronic polymeric micelles can take pharmacological action on both human umbilical vein endothelial cells and KBv MDR cancer cells, resulting in a dual-functional anticancer effect similar to that observed in our *in vitro* cellular studies.

Keywords: dual-functional, micelles, c(RGDyK), antiangiogenesis, multidrug resistance

Introduction

Cancer is a leading cause of death worldwide, and it is difficult to remove the tumor completely by conventional surgical methods. Thus, the incidence of tumor recurrence is very high due to its possible invasion into the surrounding normal tissue.^{1,2} Consequently, chemotherapy is a necessary strategy for the cancer treatment. However, poor tumor targeting with undesirable side effects as well as the emergence and development of multidrug-resistant (MDR) seriously restrict its ability to influence clinical outcome.^{3,4}

Angiogenesis is a process of generating new blood vessels in tumor sites to supply necessary oxygen and nutrients,^{5,6} which has been proved to play a vital role in tumor growth and development.^{7,8} During this process, $\alpha_v\beta_3$ integrin, a well-known angiogenesis biomarker, was detected in the activated endothelial cells and most tumor cells.⁹ The critical functions of $\alpha_v\beta_3$ integrin in cancer therapy are related to cell survival, adhesion, migration, invasion, and angiogenesis.¹⁰⁻¹² Moreover, it interacts by cross-talking with vascular endothelial growth factor (VEGF) to control tumor growth, metastasis, and angiogenesis.¹³ Due to its effects on angiogenesis process, $\alpha_v\beta_3$ integrin has been

Correspondence: Yanzuo Chen
Department of Pharmaceutics, School of Pharmacy, East China University of Science and Technology, Lane 130, Meilong Road, Shanghai 200237, People's Republic of China
Tel +86 21 6425 2449
Fax +86 21 6425 2449
Email chenyz@ecust.edu.cn

Xiaoling Fang
Key Laboratory of Smart Drug Delivery, Ministry of Education and PLA, School of Pharmacy, Fudan University, Lane 826, Zhangheng Road, Shanghai 201203, People's Republic of China
Tel +86 21 5198 0071
Fax +86 21 5198 0072
Email xlfang@shmu.edu.cn

considered as one of the most promising targets for cancer therapy⁹ and the development of drug-targeting delivery systems.¹⁴ For $\alpha_v\beta_3$ integrin targeting, the RGD (arginine-glycine-aspartic acid) short peptides have been widely used, due to their high affinity and specificity to $\alpha_v\beta_3$ integrin, as well as long half-life. Therefore, RGD peptide sequences have been applied as the ligand for the development and integrin-targeted drug and gene delivery.^{15,16}

Although angiogenesis is one of the main features of tumor growth and migration, the development of MDR becomes a serious obstacle to the effective chemotherapy.¹⁷ One of the best known mechanisms responsible for the MDR phenotype in cancer is the overexpression of P-glycoprotein (P-gp).^{18,19} Generally, P-gps act as export “pumps” for a wide range of structurally and functionally unrelated chemotherapeutic drugs such as vinca alkaloids, anthracyclines, epipodophylotoxins, and taxanes.¹⁷ Therefore, the decrease of P-gp-mediated drug efflux could be one of the most effective ways to enhance antitumor efficiency to overcome MDR. Recently, several polymeric carrier approaches have been proposed to overcome MDR in cancer chemotherapy^{20,21} among which Pluronic block copolymer has been identified as a biological response modifier that can interact with MDR cancer cells resulting in drastic sensitization of resistant tumors to anticancer drugs.²² Particularly, as reported, Pluronic P105 has acted as an inhibitor of P-gp, and several types of P105-based nanoparticles have been shown to possess MDR modulation activities. It has been also reported that drug-loaded Pluronic P105 micelle formulation can cause significant reversal of MDR in MCF-7/ADR cells, SKOV-3/PTX cells, and KBv cells in our previous studies.^{23–25} However, the in vitro stability of micelles composed of single Pluronic P105 polymer is still unsatisfied, which is mainly due to its short PEO length. To overcome this issue, Pluronic F127 with high PEO-PPO ratio was incorporated into the micelle structure in an attempt to enlarge and expand the hydrophilic layer of Pluronic micelles, and this is believed to improve the stability of Pluronic P105-based micellar system, prolong blood circulation time, and modify the biodistribution behavior of the anticancer drug.^{23,26–29} Therefore, drug-loaded Pluronic micelles fabricated with Pluronic P105 and F127 were selected as the matrix of the polymeric micelles. Furthermore, c(RGDyK) (cyclic RGD [arginine-glycine-aspartic acid] peptide)-decorated Pluronic F127 and P105 mixed micelles are developed in this study to form a dual-functional drug delivery system for the antiangiogenesis and modulation of drug resistance.

Both doxorubicin (DOX) and paclitaxel (PTX) are well-known first-line chemotherapeutic agents with excellent antitumor efficiency against a broad spectrum of solid tumors.

It has been reported that simultaneous administration of DOX and PTX to patients with metastatic breast cancer is superior to that of individual drug therapy in terms of tumor regression rates.^{30,31} However, because of the potential emergence of MDR, their clinical outcome is compromised to some extent. However, in order to modulate the MDR and further enhance the therapeutic efficacy, c(RGDyK)-decorated Pluronic micelles have been prepared to load both DOX and PTX. The dual-functional effect of this targeted Pluronic nanomicelles was evaluated in both integrin-expressed angiogenic endothelial cells (human umbilical vein endothelial cells [HUVEC]) and MDR tumor cells (KBv) in vitro-based models.

Materials and methods

Materials

Pluronic P105 and F127 were kindly provided by BASF Ltd. (Shanghai, People’s Republic of China). DOX was obtained from Beijing Huafeng United Technology Co. Ltd. (Beijing, People’s Republic of China), and PTX was purchased from Xi’an Sanjiang Bio-Engineering Co. Ltd. (Xi’an, People’s Republic of China). Free PTX solution was prepared according to the commercial formulation of Taxol. c(RGDyK) (molecular weight [MW] =619.51) was synthesized by the GL Biochem Ltd. (Shanghai, People’s Republic of China). P105-DOX was synthesized in our lab, and the synthesis and characterization of P105-DOX is provided in the supporting information (Figure S1). Compounds such as *N,N'*-dicyclohexyl carbodiimide (DCC), *N*-hydroxysuccinimide (NHS), 3-(4,5-dimethyl-thiazol-2-yl)-2,5-diphenyl-tetrazolium bromide (MTT), and Hoechst 33342 were purchased from Sigma-Aldrich (St Louis, MO, USA). Cell Cycle and Apoptosis Analysis Kits were purchased from Beyotime® Biotechnology Co. Ltd (Nantong, People’s Republic of China). Micro BCA Protein Assay Kit and Triton X-100 were purchased from Beyotime Biotechnology Co., Ltd. Penicillin–streptomycin, Dulbecco’s Modified Eagle’s Medium (DMEM), fetal bovine serum (FBS), and 0.25% (w/v) trypsin solution were purchased from Gibco BRL (Gaithersburg, MD, USA). Purified deionized water was prepared by Milli-Q plus system (Millipore Co., Billerica, MA, USA). All other reagents and chemicals were of analytical grade and were used without further purification.

The MDR human carcinoma KBv cell line was purchased from Nanjing KeyGen Biotech. Co. Ltd. (Nanjing, People’s Republic of China), with 0.2 $\mu\text{g}/\text{mL}$ of vinblastine in the cell culture medium to maintain the selective pressure. HUVEC was purchased from Chinese Academy of Sciences Cells Bank (Shanghai, People’s Republic of China) cultured in the medium containing endothelial cell growth

supplement (ScienCell, Carlsbad, CA, USA). Both the cell lines were cultured in DMEM supplemented with 10% FBS and 1% penicillin–streptomycin at 37°C in a humidified 5% CO₂–95% O₂ atmosphere. Culture plates and dishes were obtained from Corning Inc. (Corning, NY, USA).

Synthesis of c(RGDyK)-decorated Pluronic F127

Synthesis of carboxyl-terminated Pluronic F127 (F127-COOH)

Pluronic F127 (0.01 M) was dissolved in acetone (400 mL) and allowed to react at room temperature. Approximately 17 mL of Jones's reagent (containing 0.02 M CrO₃) was added to the F127 acetone solution. The reaction mixture was kept under stirring at room temperature overnight. Then, the reaction was terminated by the addition of 5 mL isopropyl alcohol followed by the addition of 12.6 g of finely powdered activated charcoal and was kept under stirring for another 4 hours; then, the mixture was filtered to get the transparent filtrate, which was subsequently precipitated by an excessive amount of cold hexane. The product, carboxyl-terminated Pluronic F127 (F127-COOH), was obtained after filtering and drying in a vacuum for 72 hours.

Synthesis of c(RGDyK)-decorated F127 (c[RGDyK]-F127)

The scheme for the synthesis of c(RGDyK)-F127 is shown in Figure 1A. Briefly, F127-COOH (0.67 g, 0.053 mM), *N,N'*-dicyclohexyl carbodiimide (0.0219 g, 0.106 mM), NHS (0.0122 g, 0.106 mM), and 5 mL of dichloromethane were added to a round-bottom flask equipped with a magnetic stirring bar, attached to a nitrogen line and a bubbler. The reaction was maintained for 24 hours at room temperature. The reaction mixture was then filtered, concentrated under reduced pressure, and precipitated in cold diethyl ether and dried under vacuum at room temperature to obtain F127-NHS.

F127-NHS (0.05 g, 0.0053 mM) dissolved in 1 mL *N,N*-dimethylformamide (DMF) was added to a solution of 6.3 mg of c(RGDyK) in 0.1 M 4-(2-hydroxyethyl)-1-piperazineethanesulfonic acid (HEPES), adjusting to pH 8.4 with *N*-methylmorpholine. The reaction was maintained for 24 hours at room temperature under moderate stirring. Following this period, the resulting reaction mixture was dialyzed against distilled water using cellulose ester membrane with a MW cutoff of 7,000 Da for 72 hours and further confirmed by the disappearance of the uncoupled peptide using the Micro BCA Protein Assay Kit. The final solution was lyophilized and stored at –20°C until further use.

Preparation and characterization of c(RGDyK)-decorated Pluronic micelles

Preparation of the micelles

The c(RGDyK)-decorated Pluronic micelle c(RGDyK)-F127/P105-DOX/PTX, abbreviated as c(RGDyK)-FP-DP, was prepared through the thin-film hydration technique according to the procedure described previously (Figure 1B).²⁷ Briefly, F127 (22.2 mg), c(RGDyK)-F127 (11.1 mg), P105-DOX (36.7 mg), P105 (230 mg), and PTX (6 mg) were dissolved in 5 mL dichloromethane. A thin polymeric film was formed in a round-bottom flask after removing the organic solvents from the aforementioned mixed solution through rotary evaporation at 37°C. The film thus formed was further dried under vacuum at room temperature overnight to remove any traces of remaining organic solvents. Then, the dry polymeric film was hydrated with 5 mL deionized water at 37°C. The mixture was stirred at 750 rpm for 30 minutes to obtain a transparent reddish micelle solution, which was then filtered through 0.22 μm membrane. Pluronic micelles without c(RGDyK) decoration (F127/P105-DOX/PTX, abbreviated as PF-DP) were prepared as described earlier, ie, without the addition of c(RGDyK)-F127, instead with an equivalent dose of F127. In addition, blank Pluronic micelles without drugs (PF and c[RGDyK]-FP) were also prepared in a similar manner for the future biocompatibility study.

It is also important to point out that DOX was used as a fluorescent agent in this study in order to monitor the intracellular fate of the Pluronic micelles. DOX-labeled blank Pluronic micelles (PF-DOX and c[RGDyK]-FP-DOX) were prepared in the same way as those of PF-DP and c(RGDyK)-FP-DP, except that the amounts of P105-DOX and P105 were 6.7 mg and 260 mg, respectively.

Characterization of c(RGDyK)-decorated Pluronic micelles

The morphology of c(RGDyK)-PF-DP was tested by transmission electron microscopy (TEM) (JMPEG-PTMC-1230; JEOL, Tokyo, Japan) and atomic force microscopy (AFM) (Veeco Instruments Inc, Plainview, NY, USA). The particle size distribution and zeta potential were measured by the dynamic light scattering method using a Zetasizer Nano ZS (Autosizer 4700; Malvern Instruments, Malvern, UK).

Drug-loading coefficient and in vitro release

The drug-loading coefficients (DL%) of PF-DP and c(RGDyK)-FP-DP were assessed by extracting with 50% acetonitrile solution (v/v) to separate free DOX and PTX from micelles, and measured using well-established high performance liquid

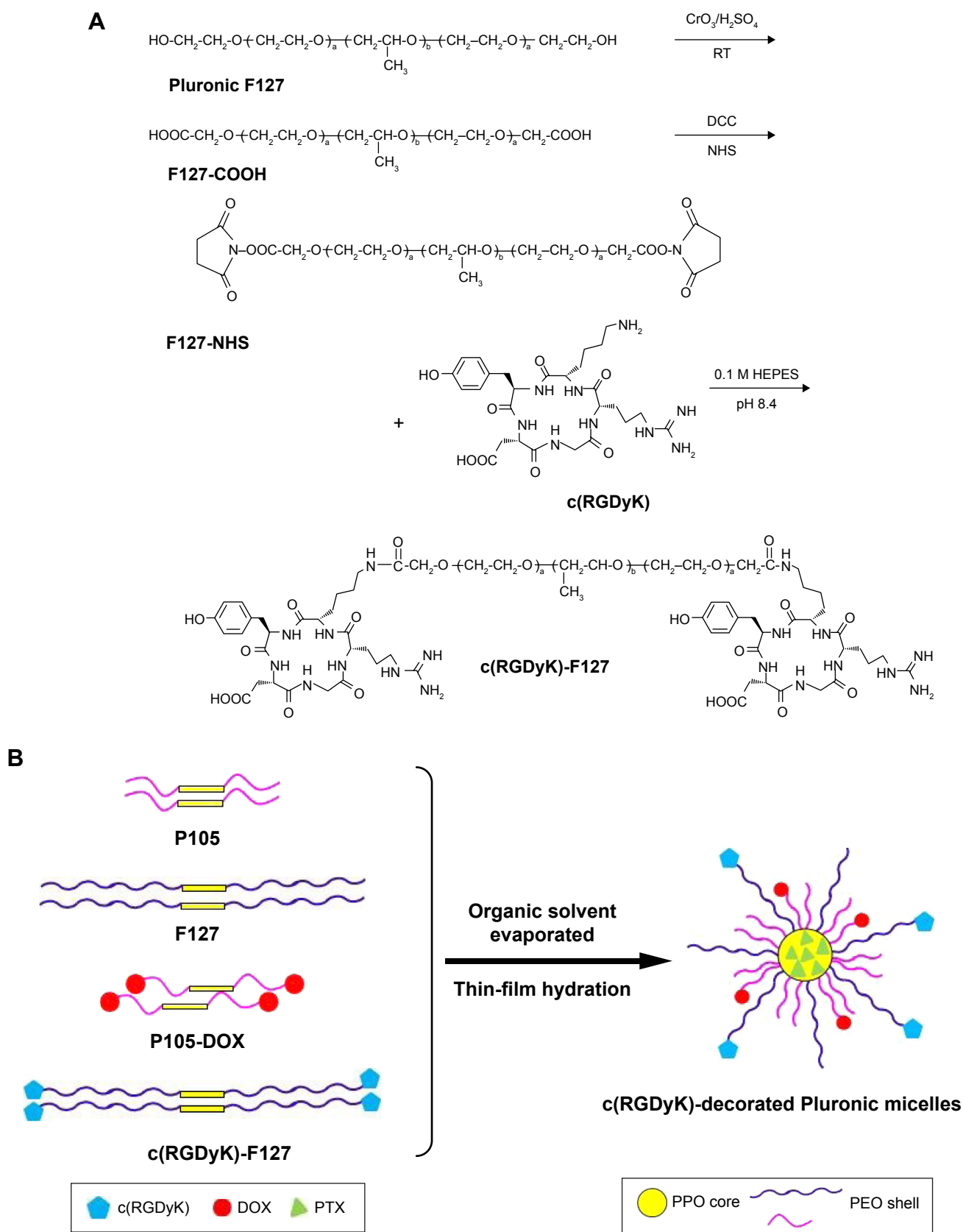


Figure 1 The schematic illustration of the c(RGDyK)-F127 synthesis and the preparation of c(RGDyK)-decorated Pluronic micelles loaded with DOX and PTX.

Notes: (A) Synthesis of c(RGDyK)-decorated Pluronic F127; (B) Schematic representation of the fabrication of c(RGDyK)-decorated Pluronic micelles loaded with DOX and PTX.

Abbreviations: c(RGDyK), cyclic RGD peptide; RGD, arginine-glycine-aspartic acid; DOX, doxorubicin; PTX, paclitaxel; RT, room temperature; DCC, dicyclohexylcarbodiimide; NHS, N-hydroxysuccinimide.

chromatography (HPLC) methods.^{28,32} The in vitro release behavior of drug from micelles was monitored in phosphate-buffered saline (PBS) (pH 5.0 or 7.4) with 0.2% Tween-80 by the dialysis method.³³ Approximately 0.2 mL aliquots were withdrawn at appropriate time intervals, followed by the supplement with equal volume of fresh medium. The concentrations of DOX and PTX in the sample were measured by HPLC.

Antiangiogenesis testing

Qualitative analysis for HUVEC cellular uptake

HUVEC cells were seeded at a density of 4×10^5 cells/well in six-well plates and incubated for 24 hours. Then, HUVEC cells were incubated with PF-DOX and c(RGDyK)-FP-DOX at a concentration of 100 $\mu\text{g/mL}$ for 0.5 hour, 1 hour, and 2 hours, or at different concentrations of 50 $\mu\text{g/mL}$, 100 $\mu\text{g/mL}$, and 200 $\mu\text{g/mL}$ for 1 hour at 37°C. The solution was removed and the cells were washed three times with ice-cold PBS (pH 7.4) and then visualized under fluorescent microscope (DMI 4000B; Leica Microsystems, Wetzlar, Germany).

For the competition assay, the c(RGDyK)-FP-DOX concentration was kept at 200 $\mu\text{g/mL}$. HUVEC cellular uptake was carried out at 37°C and 4°C. Besides, c(RGDyK) was added to the wells in advance at a concentration of 0.3 $\mu\text{g/mL}$. After incubation for 1 hour at 37°C, the compound was withdrawn from the wells, and c(RGDyK)-FP-DOX was added along with c(RGDyK) and incubated for another 1 hour. Then the solution was removed and the cells were washed three times with ice-cold PBS (pH 7.4) and then visualized under fluorescent microscope.

Quantitative analysis for HUVEC cellular uptake

For the quantitative analysis of the cellular uptake of c(RGDyK)-decorated Pluronic micelles, HUVEC cells were seeded at a density of 1×10^5 cells/well in 24-well plates, incubated for 24 hours, and checked for confluence and morphology. Then, HUVEC were incubated with PF-DOX and c(RGDyK)-FP-DOX at various concentrations (50–1,500 $\mu\text{g/mL}$) at 4°C and 37°C, respectively, or for different time intervals (0.25–4 hours) at 37°C. The cells were washed with PBS, trypsinized, centrifuged at 1,000 rpm for 5 minutes, washed, resuspended in PBS, and analyzed using a flow cytometer (FACS Calibur; BD Biosciences, San Jose, CA, USA).

Biocompatibility study

To evaluate the biocompatibility of the micelles and the effect of (RGDyK)-decorated Pluronic micelles on angiogenesis, HUVEC cells were seeded at a density of 1×10^4 cells/well in 96-well plates. After 24 hours of incubation, the medium was removed, and the cells were incubated for 72 hours in the media

containing PF and c(RGDyK)-FP at various concentrations. Cell survival was measured using MTT assay. Briefly, 180 μL of fresh growth medium and 20 μL of MTT (5 mg/mL) solution were added to each well. The plate was incubated for an additional 4 hours, and then 200 μL of dimethyl sulfoxide (DMSO) was added to each well to dissolve any purple formazan crystals formed. The plates were vigorously shaken before taking the measurement of relative color intensity. The absorbance at 570 nm of each well was measured by a microplate reader (Tecan Safire2, Switzerland).

HUVEC tubular formation assay

Approximately, HUVEC cells in 100 μL DMEM at a density of 1.5×10^4 cells/well were seeded in 96-well plate precoated with 40 μL 30% phenol red-free matrigel. After incubation for 30 minutes, VEGF (50 ng/mL) and c(RGDyK)-FP-DP and PF-DP with various carrier concentrations (1 $\mu\text{g/mL}$, 10 $\mu\text{g/mL}$, 50 $\mu\text{g/mL}$, 100 $\mu\text{g/mL}$, 500 $\mu\text{g/mL}$, and 1000 $\mu\text{g/mL}$, w/v) were treated and compared to the negative control (without VEGF or drug) and the positive control (with VEGF and without drug). After mild shaking, the plate was kept in the incubator for 12 hours. Then, branches of capillary-like tube in each well were visualized and counted under microscope (DMI 4000B; Leica) for statistical analysis.¹²

c(RGDyK)-decorated Pluronic micelles for the treatment of drug-resistant tumor cells

KBv cellular uptake study

For the study, 24-well culture plates were seeded with KBv cells at a density of 1×10^5 cells per well and incubated at 37°C for 24 hours to allow for the cell attachment. After 24 hours of incubation, the medium was replaced by 5 $\mu\text{g/mL}$ of mixture containing DOX and PTX (DOX+PTX, DOX:PTX =2:3, w/w), PF-DP, or c(RGDyK)-FP-DP in FBS-free DMEM. After 4 hours of incubation at 37°C, cells were washed twice with cold PBS and then lysed with 0.4 mL PBS containing 1% Triton X-100. After incubation, 100 μL of the cell lysate was withdrawn and extracted with methanol (200 μL /sample), and the mixture was then subjected to probe-type ultrasonic treatment (400 W, ten cycles with 2 s active 3 s duration, JY92-II; Scientz Biotechnology Co. Ltd., Ningbo, People's Republic of China) in ice bath. After extraction, the mixture was centrifuged at 5,000 rpm for 5 minutes, and the supernatant was analyzed by HPLC. The protein content in the sample was determined using the Micro BCA Protein Assay Kit in accordance with the method specified by the manufacturer. Cellular accumulation of DOX

and PTX was normalized with respect to the total protein content determined by the BCA method.

Cell apoptosis activity against KBv cells

The cell apoptosis activity was detected by the assessment of nuclear morphology in KBv cells by Hoechst 33342 staining. Briefly, cells were seeded in six-well plates containing a coverslip with 5×10^5 cells per well and cultured for 24 hours. Cells were then incubated for another 24 hours with a mixture of DOX and PTX (DOX+PTX, DOX:PTX =2:3, w/w), c(RGDyK)-FP-DP, or PF-DP (total drug concentration of 1 $\mu\text{g}/\text{mL}$), and DMEM was used as the control group. After incubation, the medium was removed and cells were fixed with 4% paraformaldehyde in PBS (pH 7.4) at room temperature for 15 minutes, stained with 10 $\mu\text{g}/\text{mL}$ Hoechst 33342 in PBS at room temperature for 15 minutes, and then washed twice with ice-cold PBS followed by the observation using fluorescent microscopy (Leica).

Cell cycle distribution

It is well-known that flow cytometry can provide information on the phases of cell cycle and is sensitive to apoptosis because the bivariate analysis method was employed for the DNA content measurement. For the analysis of cell cycle distribution, KBv cells were seeded in six-well plates and treated with mixture of DOX and PTX (DOX+PTX, DOX:PTX =2:3, w/w), PF-DP, or c(RGDyK)-FP-DP at a total drug concentration of 1 $\mu\text{g}/\text{mL}$ at 37°C for 24 hours. Cells treated with FBS-free DMEM were used as the control group. At the end of incubation, adherent and nonadherent cells were collected by trypsinization and centrifugation. Cells (1×10^6) were washed twice with ice-cold PBS, and then fixed with 70% cold ethanol at 4°C for 24 hours. Then the cells were washed twice again with cold PBS to eliminate alcohol, incubated with RNase A (100 $\mu\text{g}/\text{mL}$) for 1 hour at 37°C, and stained with propidium iodide (PI, 100 $\mu\text{g}/\text{mL}$) for another 0.5 hours in the dark prior to the cell cycle analysis.

KBv tumor spheroids penetration

In order to evaluate the influence of different formulations on the in vitro solid tumor growth, multicellular three-dimensional (3D) tumor spheroids were developed using the lipid overlay system as previously reported, which can be used as a useful tool to simulate the in vivo solid tumors. Briefly, KBv cells at a density of 2×10^4 cells/well in 500 μL DMEM were seeded in 24-well plate which was precoated with 300 μL of 2% low melting point agarose. After 1 week of incubation, PF-DOX or c(RGDyK)-FP-DOX at a final carrier concentration of 500 $\mu\text{g}/\text{mL}$ was added to the tumor

spheroids for 4 hours, and then rinsed with PBS, transferred to chambered coverslips, and analyzed using a confocal laser scanning microscopy (TCS SP5; Leica). Z-stack images were obtained by scanning the tumor spheroid step-by-step. The scanning began from the top of a spheroid. Each scanning layer was 30 μm in thickness, and the total scanning was done upto a depth of 90 μm in a spheroid.

Dual-functional effect in vitro

In order to evaluate the dual-functional effect of c(RGDyK)-modified micelles in vitro, HUVEC–KBv tumor spheroids coculture model was established.³⁴ HUVEC cells were seeded on polycarbonate 24-well transwell membrane with 1.0 μm mean pore size and 0.33 cm^2 surface area (FALCON Cell Culture Insert; Becton Dickinson Labware, Franklin Lakes, NJ, USA) at a density of 5×10^4 cells/well. The transepithelial electric resistance was recorded daily. When the transepithelial electric resistance was sustained over 200 Ω , transwells were selected for the experiment.³⁵ The selected transwell was inserted into another 24-well culture plate with KBv tumor spheroids being cultured for 1 week. The cells in the transwell chambers were cocultured for another 24 hours prior to use.³⁵ The serum-free DMEM containing a mixture of DOX and PTX (DOX+PTX, DOX:PTX =2:3, w/w), PF-DP, or c(RGDyK)-FP-DP (500 $\mu\text{g}/\text{mL}$) was applied to the apical chamber of the transwell system. Cocultured cells were exposed to the treatment for 12 hours. Then, the transwell insert was removed, and KBv tumor spheroids were cultured for another 7 days. Tumor spheroids incubated in only DMEM were used as the control group. After different treatments, tumor spheroids were observed under an inverted microscope (Chongqing Optical & Electrical Instrument Co. Ltd., Chongqing, People's Republic of China) every day. The major (d_{max}) and minor (d_{min}) diameter of each selected spheroid were determined and the corresponding spheroid volume (V) was calculated using Equation 1:

$$V = \frac{\pi \times d_{\text{max}} \times d_{\text{min}}}{6} \quad (1)$$

The tumor spheroid volume ratio (R) was calculated using Equation 2:

$$R = \frac{V_i}{V_0} \times 100\% \quad (2)$$

where V_i is the KBv tumor spheroid volume at the i th day after treatment, and V_0 is the tumor spheroid volume prior to the treatment.

Results and discussion

Characterization of c(RGDyK)-F127

As shown in $^1\text{H-NMR}$ spectrum, the solvent peak of CDCl_3 was found at 7.25 ppm (Figure 2A and C) and of DMSO-d_6 was found at 2.48 ppm (Figure 2B). The peaks at 1.14 ppm and 3.40–3.60 ppm were attributed to $-\text{CH}_3$ of PPO and $-\text{CH}_2\text{CHO}$ of PPO and PEO in F127, respectively. As shown in Figure 2B, F127-COOH copolymer was activated by the reaction with NHS. The characteristic peak at 2.52 ppm was assigned to the protons of the NHS unit, indicating the addition of NHS to the PEO terminus. The excessive c(RGDyK) was removed by dialysis against deionized water. There was a characteristic peak of the $-\text{CH}_2-\text{CH}_2-$ group in c(RGDyK) at 2.17 ppm (Figure 2C). The yield of F127-COOH, F127-NHS, and c(RGDyK)-F127 was 75.9%, 83.4%, and 89.2%, respectively. The conjugation percentage of c(RGDyK) to Pluronic F127 was 91.44% on a molar ratio basis.

Characterization of c(RGDyK)-decorated Pluronic micelles

The mean diameter of both c(RGDyK)-FP-DP and PF-DP was found to be approximately 23 nm, with an acceptably good polydispersity index ($\text{PDI} < 0.2$). Such micelles may accumulate in the tumor due to the enhanced permeability and retention effect.³⁶ The particle size observed by TEM and AFM images were in good correspondence with that measured by the laser scattering technique (Figure 3A and B). The surface charge values were close to neutral (within ± 5 mV). It was also found that there is no significant difference in drug-loading coefficient between c(RGDyK)-FP-DP and PF-DP (Table 1).

The in vitro cumulative release profiles of DOX and PTX from PF-DP and c(RGDyK)-FP-DP at pH 5.0 and pH 7.4 are shown in Figure 3C. Similar to PF-DP, the sustained release of DOX and PTX for over 72 hours was observed in c(RGDyK)-FP-DP at neutral pH. In contrast with the release profiles at pH 7.4, both DOX and PTX release rate increased in pH 5.0 buffer, and the release rates of DOX and PTX during 72 hours were 45.9% and 75.6% for PF-DP, and 47.4% and 73.9% for c(RGDyK)-FP-DP, respectively, suggesting that the simulated acidic environment in the lysosome might facilitate the drug release from polymeric micelles.³⁷ The results suggest that moderate modification of c(RGDyK) did not significantly influence the DOX and PTX release behavior.

Antiangiogenesis test

Qualitative analysis for HUVEC cellular uptake

DOX was used as a fluorescence probe to label blank micelles for cellular uptake test, the results of which were shown

qualitatively by fluorescent images. HUVEC cells treated with either PF-DOX or c(RGDyK)-FP-DOX exhibited variable fluorescent intensity depending on the concentration of micelles (Figure 4A) and the incubation time (Figure 4B). The cellular uptake of c(RGDyK)-FP-DOX in HUVEC cells exhibited concentration- and time-dependent mode, and was higher than those of FP-DOX when the concentration of micelles ranged from 50 $\mu\text{g/mL}$ to 200 $\mu\text{g/mL}$ or the incubation time ranged from 0.5 hour to 2 hours at an identical micelle concentration. Cellular uptake of c(RGDyK)-FP-DOX at 4°C by HUVEC cells was much lower when compared to that at 37°C (Figure 4C). In addition, it was found that after adding free c(RGDyK) peptide, cellular uptake of c(RGDyK)-FP-DOX was reduced (data not shown). Therefore, the cellular uptake of c(RGDyK)-FP-DOX exhibited a concentration-, time- and energy-dependent mode. On preconditioning with c(RGDyK) peptide, ligands of integrin, the cellular uptake of c(RGDyK)-FP-DP was reduced, probably due to the fact that integrin can competitively bind with the free ligands.

Quantitative analysis for HUVEC cellular uptake

The cellular uptake of the micelles was quantitatively monitored using a flow cytometer (FACS Calibur; BD Biosciences). Results showed that when the concentration of micelles ranged from 50 $\mu\text{g/mL}$ to 1,500 $\mu\text{g/mL}$, the mean fluorescence intensity of DOX in c(RGDyK)-FP-DOX group was found to be much higher than that in PF-DOX group in HUVEC cells at 37°C ($P < 0.05$). Additionally, the mean fluorescence intensity of both c(RGDyK)-FP-DOX and PF-DOX significantly decreased at 4°C ($P < 0.05$), compared with that at 37°C (Figure 4D). The effect of incubation time on cellular uptake of c(RGDyK)-FP-DOX was also evaluated (Figure 4E). It was found that cellular uptake of c(RGDyK)-FP-DOX was higher than that of PF-DOX at 0.5-hour, 1-hour, 2-hour, and 4-hour time points ($P < 0.05$), and both micelles exhibited a time-dependent cellular internalization.

Collectively, both qualitative and quantitative results indicated that the cellular uptake of Pluronic micelles in HUVEC cells can be increased using c(RGDyK)-decorated targeting micelles. The internalization of Pluronic micelles in HUVEC cells was found to be concentration-, time-, and energy-dependent.

Biocompatibility study

The biocompatibility of blank PF and c(RGDyK)-FP to HUVEC cells was evaluated using MTT assay (Figure 5A). The results showed that when the concentration ranged from 10 $\mu\text{g/mL}$ to 1000 $\mu\text{g/mL}$, the cytotoxicity of the two micelles

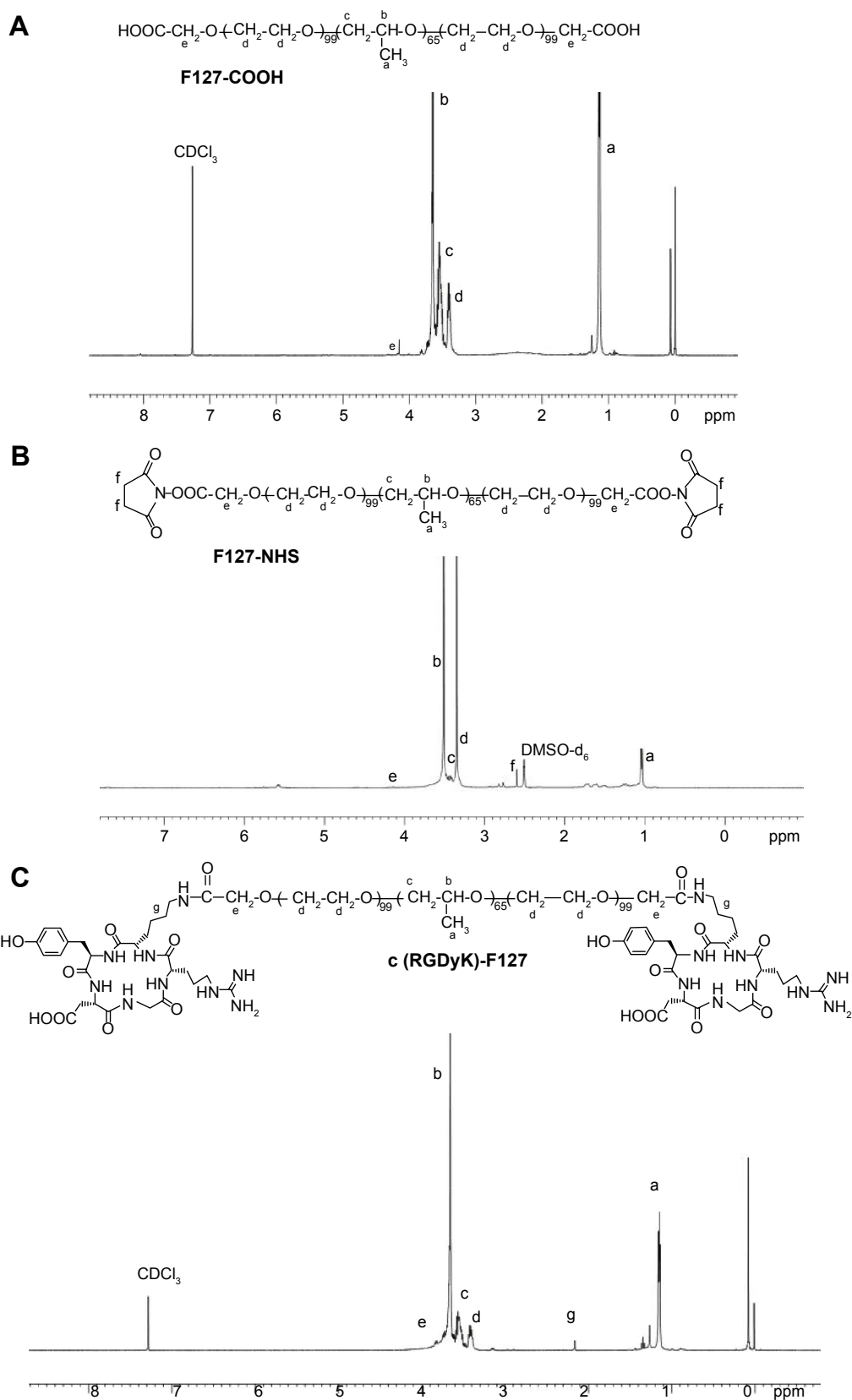


Figure 2 The $^1\text{H-NMR}$ spectra of F127-COOH, F127-NHS and c(RGDyK)-F127.

Notes: (A) $^1\text{H-NMR}$ spectra of F127-COOH; (B) F127-NHS; (C) c(RGDyK)-F127.

Abbreviations: $^1\text{H-NMR}$, $^1\text{H-nuclear magnetic resonance spectroscopy}$; NHS, *N*-hydroxysuccinimide; c(RGDyK), cyclic RGD peptide; RGD, arginine-glycine-aspartic acid; DMSO, dimethyl sulfoxide.

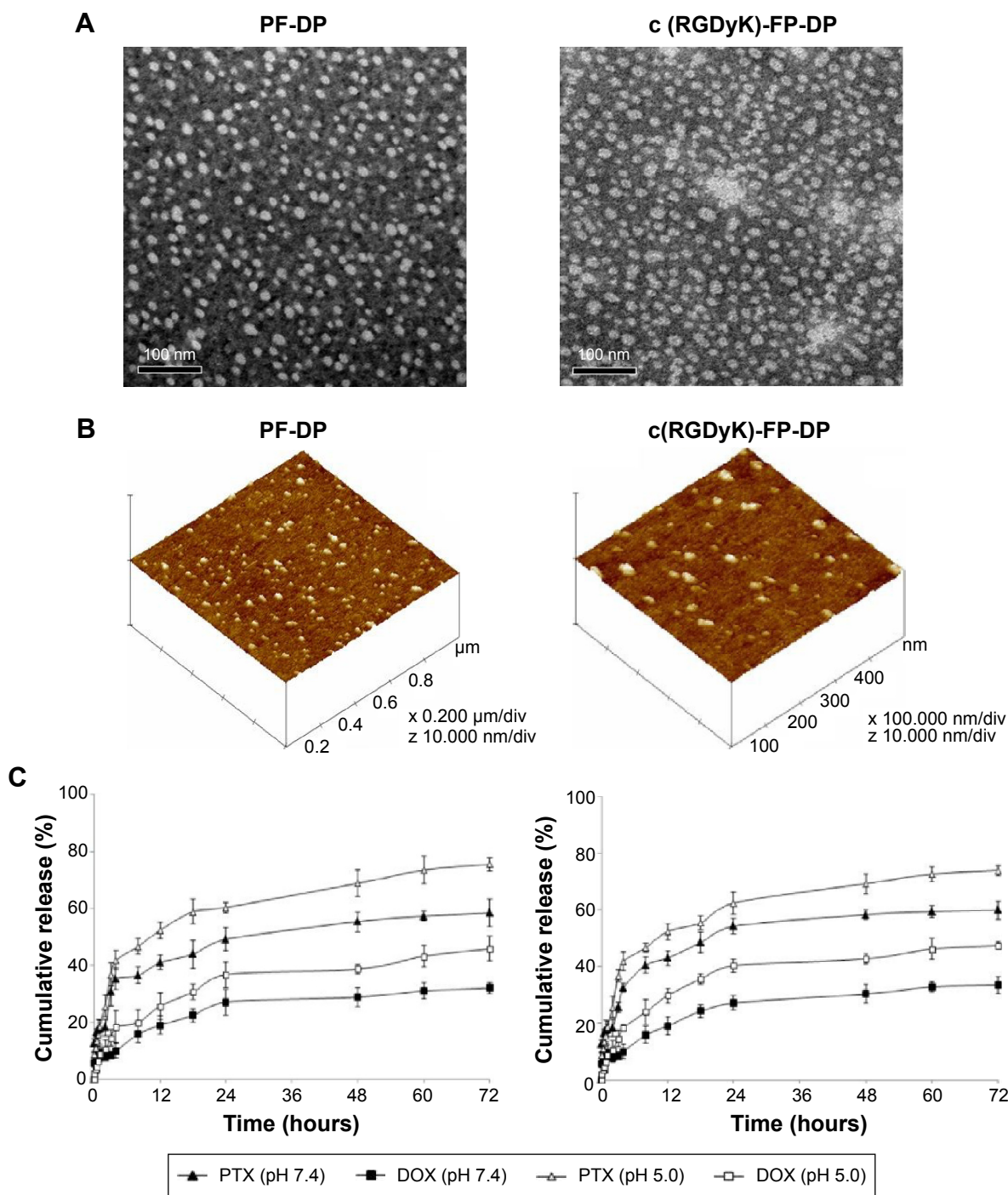


Figure 3 The characterization of PF-DP and c(RGDyK)-FP-DP micelles.

Notes: (A) Transmission electron microscopy and (B) atomic force microscopy images of PF-DP and c(RGDyK)-FP-DP; (C) In vitro release of DOX and PTX from drug-loaded Pluronic micelles in phosphate buffered saline (pH 5.0 or 7.4) media with 0.2% Tween-80.

Abbreviations: DOX, doxorubicin; PTX, paclitaxel; PF-DP, Pluronic micelles loaded with DOX and PTX; c(RGDyK)-FP-DP, c(RGDyK)-decorated Pluronic micelles loaded with DOX and PTX; c(RGDyK), cyclic RGD peptide; RGD, arginine-glycine-aspartic acid.

was negligible in HUVEC cells. Micelles displayed increasing cellular growth inhibitory effects as the concentration increased from 1,000 $\mu\text{g/mL}$ to 5,000 $\mu\text{g/mL}$, probably due to the cytostatic action of Pluronic micelles.³⁸ This phenomenon can be partially attributed to the increasing amounts of Pluronic P105,

since previous reports indicated that the increasing concentrations of Pluronic P105 increased cytotoxicity in KB, KBv, and HEK-293 cells.^{32,38} In addition, c(RGDyK)-FP was found to display higher cytotoxic effect than that of PF micelles when the concentration ranged from 10 $\mu\text{g/mL}$ to 1000 $\mu\text{g/mL}$, since

Table 1 Physicochemical characteristics of drug-loaded micelles with or without c(RGDyK) peptide decoration

Micelles	Size (nm)	Zeta potential (mV)	DOX DL (%)	PTX DL (%)
PF-DP	22.26±0.34	-1.48±0.19	1.03±0.24	1.52±0.16
c(RGDyK)-FP	22.88±0.19	-1.56±0.25	-	-
c(RGDyK)-FP-DP	23.02±0.23	-4.43±0.36	1.01±0.15	1.54±0.24

Note: Mean ± SD (n=3).

Abbreviations: c(RGDyK), cyclic RGD peptide; RGD, arginine-glycine-aspartic acid; DOX, doxorubicin; PTX, paclitaxel; DL%, drug-loading coefficient; PF-DP, Pluronic micelles loaded with DOX and PTX; c(RGDyK)-FP, c(RGDyK)-decorated Pluronic micelles loaded with PTX; c(RGDyK)-FP-DP, c(RGDyK)-decorated Pluronic micelles loaded with DOX and PTX; SD, standard deviation.

c(RGDyK) peptide could facilitate c(RGDyK)-FP accumulation into the integrin protein-rich HUVEC cells and thus facilitate the intracellular uptake.

Tubular formation of HUVEC

The ability of HUVEC to form the capillary-like tubular structure in the reconstituted extracellular matrix, in the presence of vital growth factors, was determined to be a characteristic of the later stages of angiogenesis.^{39,40} The formation of tube-like structure by HUVEC cells after 12 hours of incubation was served as a positive control. To quantify the activity of c(RGDyK)-FP-DP, the number of tubes in each well was counted per 40× field (Figure 5B). It was found that when the concentration of c(RGDyK)-FP-DP was as low as 10 µg/mL, HUVEC could not properly form the capillary structure. At the concentration of 100 µg/mL, c(RGDyK)-FP-DP completely suppressed the formation of tubular structure. As for PF-DP group, the inhibition ability of capillary-like tube formation was only observed when the concentration was administered at a concentration higher than 100 µg/mL. Thus Pluronic micelles decorated with c(RGDyK) peptide exhibited stronger inhibition potency toward tubular formation than nondecorated micelles ($P < 0.01$) at the concentration more than 50 µg/mL, probably due to the increased active cellular uptake.

Effect of c(RGDyK)-decorated Pluronic micelles on the MDR KBv tumor cells

Cellular uptake

The intracellular accumulation of DOX and PTX was determined in KBv MDR tumor cells. As shown in Figure 6, the uptake amount of DOX and PTX of c(RGDyK)-FP-DP were found to be much higher than those of PF-DP in KBv cells ($P < 0.01$). In addition, the drug cellular accumulation of Pluronic polymeric micelles was comparable to that of the P-gp inhibitor (cyclosporin A [CsA]) group ($P < 0.05$), suggesting that Pluronic P105/F127 mixed micelles have the ability to enhance drug accumulation in MDR tumor cells possibly due to the presence of Pluronic unimers.⁴¹

Moreover, the results demonstrated that the enhanced cellular uptake of c(RGDyK)-FP-DP may be in part attributed to the c(RGDyK) active targeting since integrin receptor is overexpressed in solid tumor cells.⁴² However, further experiments need to be conducted to test the integrin receptor expression in KBv cells. The same trend was also found in HUVEC-based studies, as integrin is overexpressed on the surface of HUVEC cells.⁴³

Cell apoptosis

In order to verify the effect of c(RGDyK)-decorated Pluronic polymeric micelles on cell apoptosis, Hoechst 33342 staining method was used to qualitatively track the c(RGDyK)-FP-DP-induced apoptotic cell death. The nuclei of untreated KBv cells showed homogenous fluorescence with no evidence of segmentation and fragmentation after staining (Figure 7A). After treatment with the mixture of free DOX and PTX (DOX+PTX) with total drug concentration of 1 µg/mL, only slight apoptosis took place in KBv cells, which is consistent with the studies reporting that DOX and PTX are the substrates of P-gp, multidrug resistance-associated protein, and breast cancer-resistant protein.^{41,43-45} In contrast, after 24-hour treatment, the cell nuclei became severely fragmented and segmented into dense nuclear parts in the drug-loaded Pluronic polymeric micelles group. Compared with PF-DP, c(RGDyK)-FP-DP was found to induce more severe fragmentation of the cell nuclei as shown in Figure 7A. These results indicated that c(RGDyK)-FP-DP displayed higher apoptosis induction activity in KBv cells, probably due to the increased cellular uptake of DOX and PTX imparted by the active targeting and MDR modulation.

Cell cycle analysis

To further study the effect of (RGDyK)-modified micelles on the cell cycle progression in KBv cells, cell cycle analysis was conducted using flow cytometry technique (FACS Calibur; BD Biosciences). The impact of drug-loaded micelles on the various phases of the cell cycle after the treatment with DOX+PTX, PF-DP, and c(RGDyK)-FP-DP

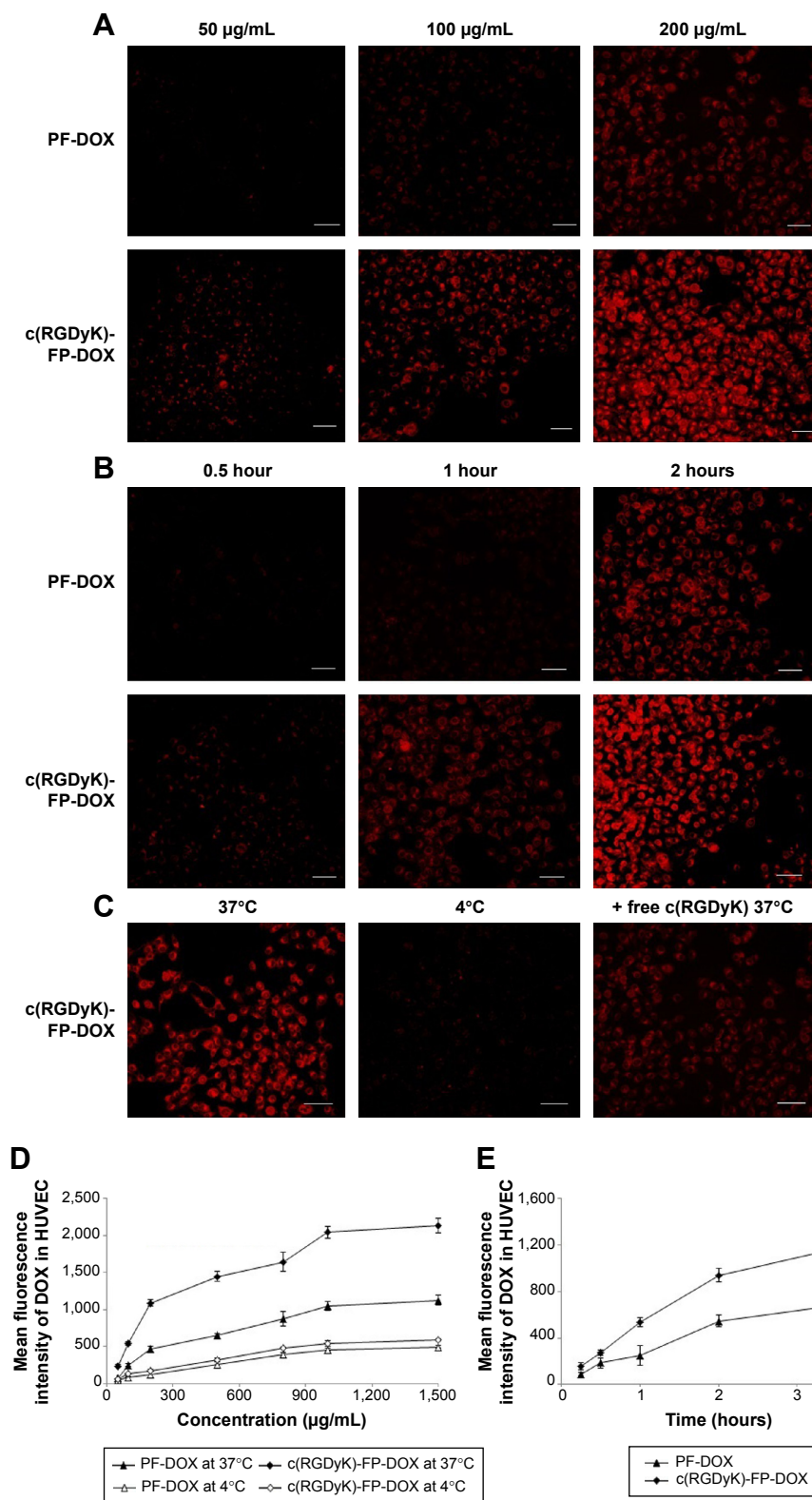


Figure 4 The qualitative and quantitative analysis for HUVEC cellular uptake.

Notes: (A) Qualitative analysis for HUVEC cellular uptake of PF-DOX and c(RGDyK)-FP-DOX at various concentrations; (B) under different incubation times; (C) when preincubated with free c(RGDyK) or incubated at 4°C; (D) quantitative analysis for HUVEC uptake when treated with 50–1,500 µg/mL c(RGDyK)-FP-DOX and PF-DOX at 37°C or 4°C for 60 minutes, respectively; (E) HUVEC uptake when exposed to 100 µg/mL c(RGDyK)-FP-DP and PF-DP at 37°C for different times. Mean ± SD (n=3). Cells were examined by fluorescent microscopy; Red: DOX; Bar: 30 µm.

Abbreviations: HUVEC, human umbilical vein endothelial cells; PF-DOX, Pluronic micelles loaded with DOX; c(RGDyK), cyclic RGD peptide; RGD, arginine-glycine-aspartic acid; c(RGDyK)-FP-DOX, c(RGDyK)-decorated Pluronic micelles loaded with DOX; c(RGDyK)-FP-DP, c(RGDyK)-decorated Pluronic micelles loaded with DOX and PTX; PF-DP, Pluronic micelles loaded with DOX and PTX; DOX, doxorubicin; PTX, paclitaxel.

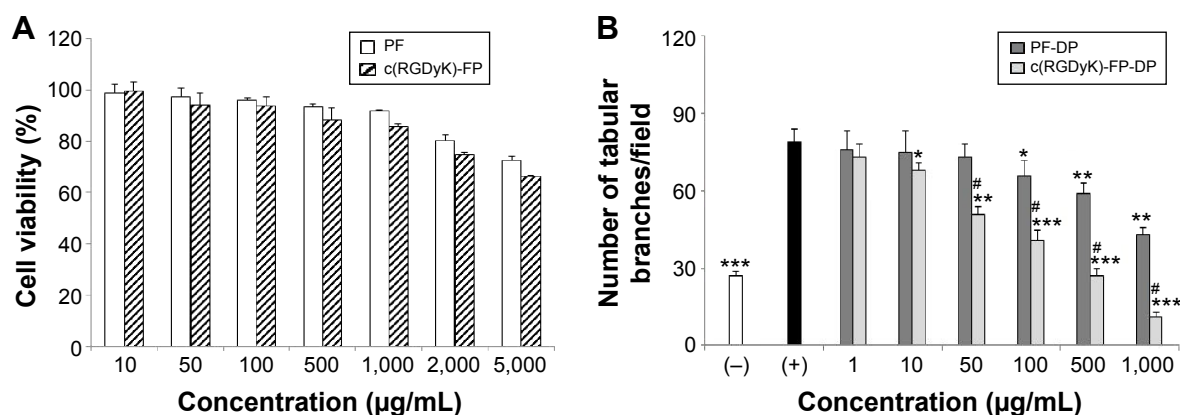


Figure 5 The biocompatibility of blank PF and c(RGDyK)-FP to HUVEC cells and the in vitro antiangiogenesis of efficacy drug loaded micelles.

Notes: (A) Cell viability of HUVEC as a function of varying concentrations of micelles at 72 hours. (B) The number of branches in the presence of varied carrier concentrations of PF-DP and c(RGDyK)-FP-DP (1 µg/mL, 10 µg/mL, 50 µg/mL, 100 µg/mL, 500 µg/mL and 1,000 µg/mL, w/v). Mean \pm SD (n=3). * P <0.05, ** P <0.01, and *** P <0.001 are compared with positive control group; # P <0.01 compared with PF-DP. Magnification is 40 \times .

Abbreviations: HUVEC, human umbilical vein endothelial cells; PF-DP, Pluronic micelles loaded with DOX and PTX; c(RGDyK)-FP-DP, c(RGDyK)-decorated Pluronic micelles loaded with DOX and PTX; c(RGDyK), cyclic RGD peptide; RGD, arginine-glycine-aspartic acid; DOX, doxorubicin; PTX, paclitaxel; SD, standard deviation.

is shown in Figure 7B and Table 2. The results indicated that after 24-hour incubation, c(RGDyK)-functionalized micelles revealed the strongest ability in arresting KBv cells in the G₂/M phase when compared with DOX+PTX and PF-DP. The boosted G₂/M phase arrest observed in the c(RGDyK)-FP-DP group was in good agreement with cell apoptosis and cellular uptake studies.

KBv tumor spheroids penetration study

There are hypoxic and avascular tumor regions in most of the solid tumors. For a cancer treatment to be curative, the drug delivery system must efficiently penetrate the tumor tissue to reach all of the viable cells. The ex vivo 3D tumor spheroids generated by liquid overlay technique are not only aggregates of cells in close contact but also contain

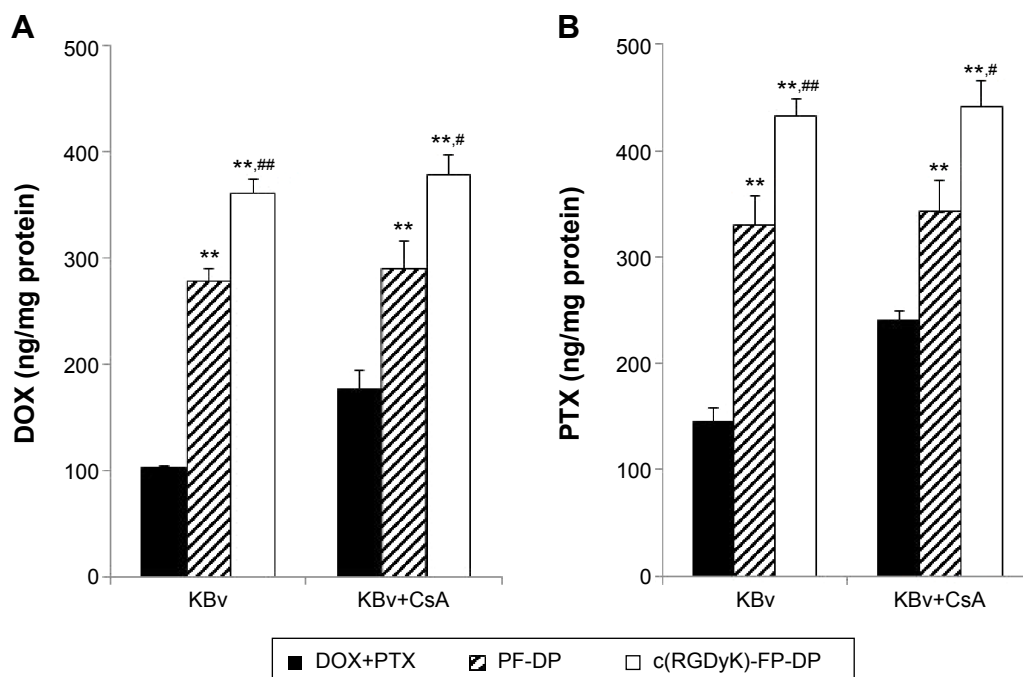


Figure 6 Cellular uptake of mixture of free DOX and PTX (DOX:PTX=2:3, w/w), PF-DP, and c(RGDyK)-FP-DP at equivalent total drug concentration (5 µg/mL) after incubation for 2 hours at 37°C in KBv cells with 5 µM CsA.

Notes: Mean \pm SD (n=3). ** P <0.01 is compared with DOX+PTX treatment; # P <0.05 and ### P <0.01 are compared with PF-DP treatment.

Abbreviations: DOX, doxorubicin; PTX, paclitaxel; PF-DP, Pluronic micelles loaded with DOX and PTX; c(RGDyK)-FP-DP, c(RGDyK)-decorated Pluronic micelles loaded with DOX and PTX; CsA, cyclosporin A; c(RGDyK), cyclic RGD peptide; RGD, arginine-glycine-aspartic acid; SD, standard deviation.

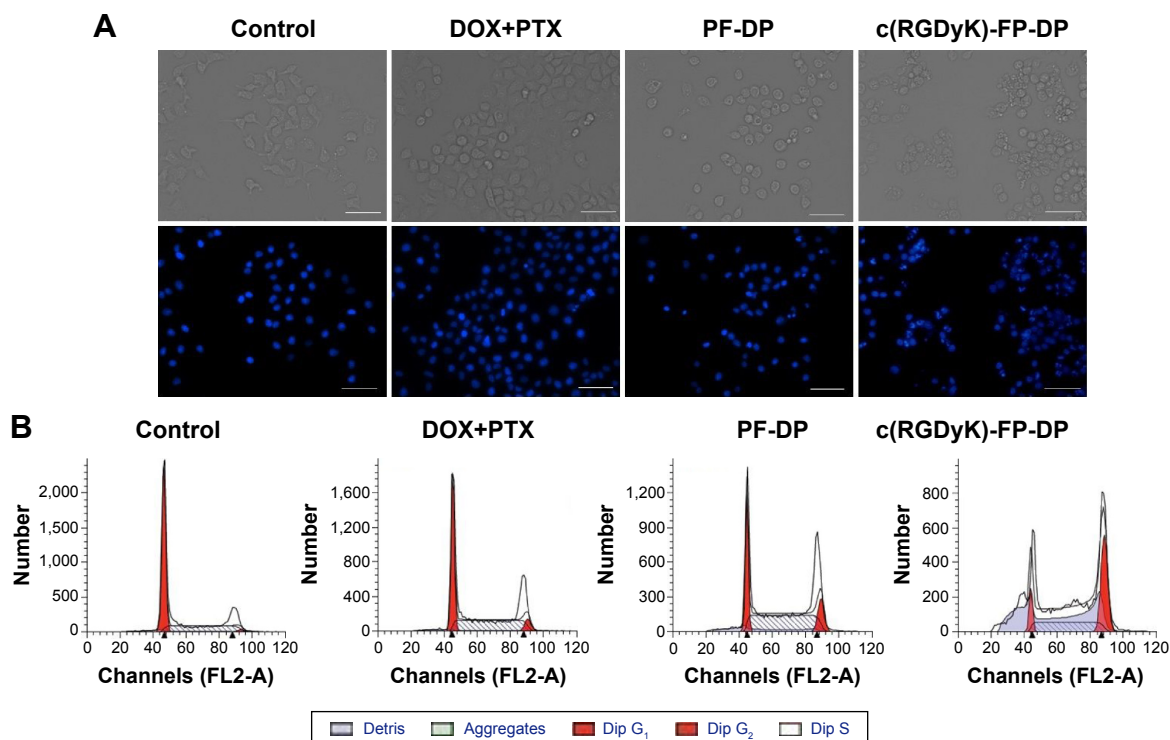


Figure 7 Cell apoptosis and cell cycle analysis in KBv cells of different formulations.

Notes: (A) Induction of apoptosis images in KBv cells by mixture of free DOX and PTX (DOX+PTX, DOX:PTX =2:3, w/w), PF-DP, c(RGDyK)-FP-DP, and control using microscopy technique. Bright field and fluorescence micrographs of KBv cell nuclei were recorded following 24-hour incubation with PF-DP and c(RGDyK)-FP-DP at the equivalent total drug concentration (1 $\mu\text{g}/\text{mL}$). (B) Flow cytometric analysis of cell cycle distribution of KBv cells after the treatment with control, DOX+PTX, PF-DP, and c(RGDyK)-FP-DP for 24 hours at the equivalent total drug concentration (1 $\mu\text{g}/\text{mL}$). Magnification is 20 \times ; the bar is 50 μm .

Abbreviations: DOX, doxorubicin; PTX, paclitaxel; PF-DP, Pluronic micelles loaded with DOX and PTX; c(RGDyK)-FP-DP, c(RGDyK)-decorated Pluronic micelles loaded with DOX and PTX; c(RGDyK), cyclic RGD peptide; RGD, arginine-glycine-aspartic acid.

an organized extracellular matrix consisting of fibronectin, laminin, collagen, and glycosaminoglycan, suggestive of the extracellular matrix of tumors *in vivo*.^{46–48} Thereby, 3D multicellular model represents the avascular regions similar to those found in many solid tumor tissues, and can serve as an invaluable tool to evaluate the effect of drug delivery system on solid tumor therapy.⁴⁹ In this study, interstitial penetration and diffusion behavior of drug-loaded micelles was tested, and the growth inhibition effect of c(RGDyK)-decorated Pluronic micelles on avascular regions of the drug-resistant solid tumors was evaluated using the

ex vivo KBv tumor spheroid model. Figure 8 shows confocal laser scanning microscopic images of KBv tumor spheroids after the treatment with DOX-labeled micelles. For the non-decorated micelles, red fluorescence of DOX was observed primarily on the periphery of tumor spheroids. However, after the application of micelles decorated with c(RGDyK) peptide, the red fluorescence was able to be observed throughout the whole tumor spheroid and the depth of fluorescence that could be observed in the spheroid can reach upto 90 μm , suggesting that micelles modified with c(RGDyK) exhibited a better capability of enhancing the spheroid penetration.

Table 2 Effect of treatment with PF-DP or c(RGDyK)-FP-DP (equivalent drug concentration at 1 $\mu\text{g}/\text{mL}$) for 24 hours on cell cycle of KBv cells

Treatment	Cell cycle distribution (%)		
	G ₀ /G ₁	S	G ₂ /M
Control	57.57±2.05	37.98±0.65	2.48±0.33
DOX+PTX	42.56±3.22	51.01±4.01	6.43±1.68
PF-DP	28.70±2.45 ^a	58.33±5.48	13.34±1.14 ^a
c(RGDyK)-FP-DP	11.50±0.72 ^{a,b}	41.39±5.33 ^{a,b}	47.11±4.38 ^{a,b}

Notes: Mean \pm SD (n=3). ^aP<0.05, compared with DOX+PTX; ^bP<0.05, compared with PF-DP.

Abbreviations: DOX, doxorubicin; PTX, paclitaxel; PF-DP, Pluronic micelles loaded with DOX and PTX; c(RGDyK)-FP-DP, c(RGDyK)-decorated Pluronic micelles loaded with DOX and PTX; RGD, arginine-glycine-aspartic acid; SD, standard deviation.

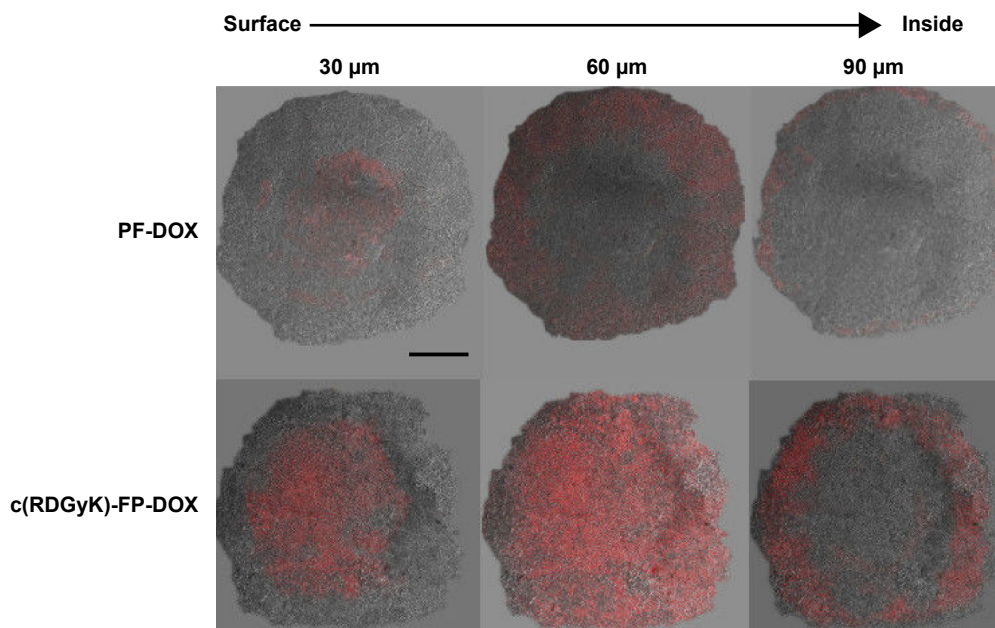


Figure 8 Penetration of PF-DOX and c(RGDyK)-FP-DOX throughout the KBv tumor spheroids.

Notes: The distribution of DOX was analyzed by confocal microscopy using Z-stack imaging with 30 μm intervals, merges of fluorescence, and DIC are shown. Scale bar represents 100 μm .

Abbreviations: PF-DOX, Pluronic micelles loaded with DOX; c(RGDyK)-FP-DOX, c(RGDyK)-decorated Pluronic micelles loaded with DOX; DIC, differential interference contrast microscopy; c(RGDyK), cyclic RGD peptide; RGD, arginine-glycine-aspartic acid.

In vitro dual-functional effects

In order to analyze the potential dual-functional effect of c(RGDyK)-FP-DP and to mimic the in vivo blood–tumor barrier, an in vitro HUVEC cells–KBv tumor spheroids coculture model was established and used for evaluation (Figure 9A).³⁴ The growth inhibition of KBv tumor spheroids by drug-loaded micelles was tested in this study. As shown in Figure 9B, KBv tumor spheroids that did not receive treatment with free DOX and PTX mixture grew fast with clearly observable 3D structure. After applying PF-DP and c(RGDyK)-FP-DP, the tumor spheroids became more and more disintegrated and shrunk over time. As observed, the cells started dissociating from the main part of spheroids from day 1 after the micelle treatment, and the 3D structure also started to disappear over the treatment period. Figure 9C shows that the change ratios (of the control, %) of KBv tumor spheroid volumes after the treatment with free DOX, PTX mixture (DOX+PTX), PF-DP, and c(RGDyK)-FP-DP every other day, respectively. It was observed that KBv tumor spheroids continued to grow in volume in the absence of drug (127.4% of the control after 7 days). DOX+PTX treatment for 7 days did not lead to significant change in volume (109.6%). As for PF-DP, significant reduction in the volume of tumor spheroids was observed after treatment for 7 days (79.82%, $P < 0.05$ compared to the control group), demonstrating the

MDR modulation capacity of Pluronic-based micelles in tumors. For c(RGDyK)-FP-DP group, the spheroids became disintegrated and almost lost the 3D structure. The inhibition effect on spheroid volume was found to be superior in PF-DP group from 3 days of treatment ($P < 0.05$), and the ultimate change ratio of KBv tumor spheroid volumes in c(RGDyK)-FP-DP group after 7 days of treatment was 54.3%, indicating that c(RGDyK)-FP-DP displayed higher transportation ability across the HUVEC cell monolayer model and stronger inhibitory effects on KBv tumor spheroids when compared with PF-DP, which was well consistent with the results of cellular uptake, tubular formation inhibition in HUVEC cells, and cell apoptosis studies.

Since the HUVEC cell monolayer has been reported to be used for simulation of the neovascular structure in solid tumors,⁵⁰ and the KBv tumor spheroids can be used to mimic the microenvironment of in vivo malignant MDR tumor, the observed relatively higher inhibitory effect in c(RGDyK)-FP-DP group using the HUVEC cells–KBv tumor spheroids coculture model suggested that micelles modified with c(RGDyK) targeting ligand exhibited a dual-functional potency, including the ability to facilitate the transportation of micelles across blood–tumor barrier and improving the therapeutic effect as observed in KBv MDR tumor cells.

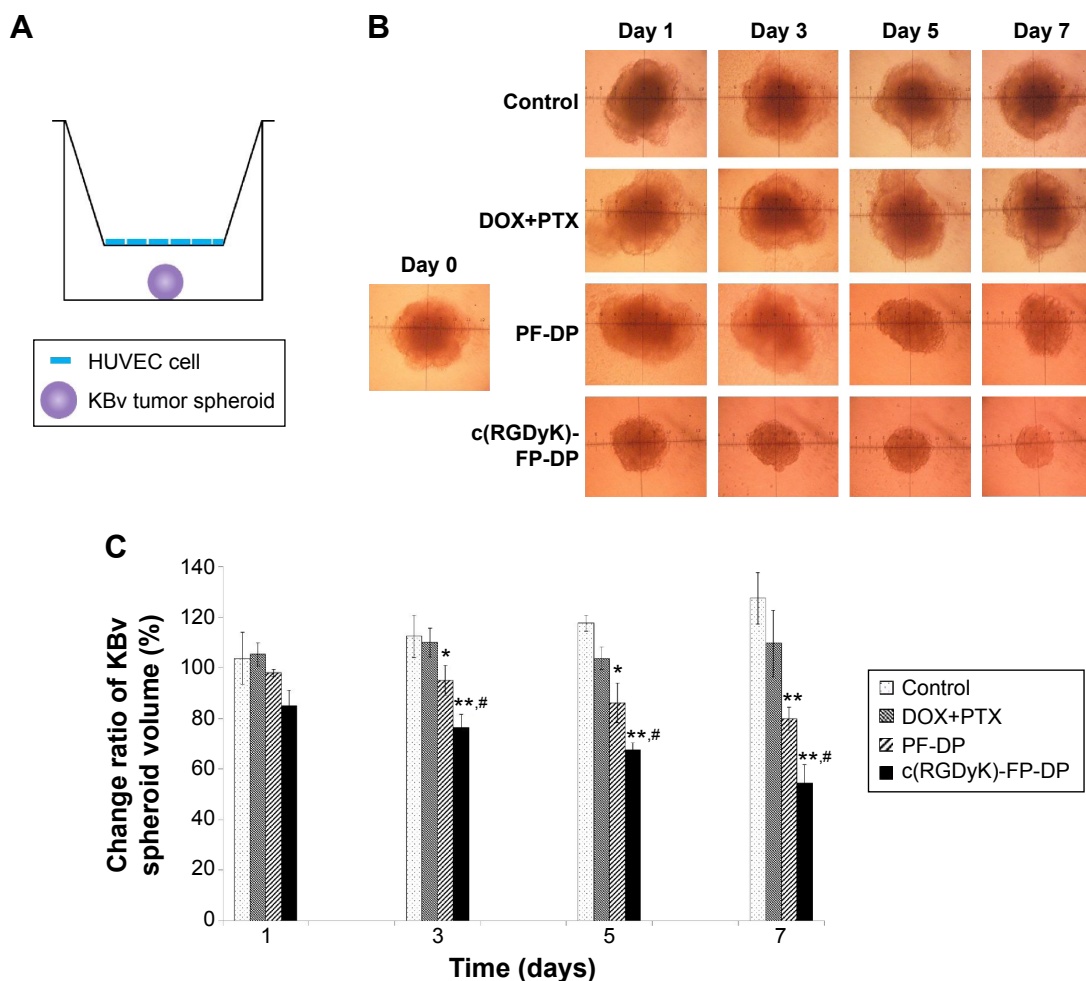


Figure 9 For evaluating the dual-function effect of c(RGDyK)-modified micelles in vitro, the HUVEC cells–KBv tumor spheroids coculture model was established.

Notes: (A) The elucidation of the HUVEC cells–KBv tumor spheroids coculture model in this study. (B) Representative confocal images of KBv tumor spheroids by the treatment with DOX+PTX, PF-DP, c(RGDyK)-FP-DP, and the control group on day 0, 1, 3, 5, and 7. (C) The ratio change in KBv spheroid volume (%) after the treatment with DOX+PTX, PF-DP, and c(RGDyK)-FP-DP. Mean \pm SD (n=3); * P <0.05 and ** P <0.01, compared with DOX+PTX group; # P <0.05, compared with PF-DP.

Abbreviations: HUVEC, human umbilical vein endothelial cells; DOX, doxorubicin; PTX, paclitaxel; PF-DP, Pluronic micelles loaded with DOX and PTX; c(RGDyK)-FP-DP, c(RGDyK)-decorated Pluronic micelles loaded with DOX; c(RGDyK), cyclic RGD peptide; RGD, arginine-glycine-aspartic acid; SD, standard deviation.

Conclusion

c(RGDyK)-decorated Pluronic micelles designed and fabricated in this study were uniformly spherical in shape with a particle size approximately 23 nm, and the release profiles of DOX and PTX in the micelles showed that they were long-acting (over 72 hours) and pH-dependent. The cellular uptake of c(RGDyK)-decorated Pluronic micelles in HUVEC cells was found to be concentration-, time-, and energy-dependent. Without causing any cytotoxicity to HUVEC cells, c(RGDyK)-FP-DP was found to possess a higher antiangiogenic efficiency than that of non-c(RGDyK)-decorated micelles. c(RGDyK) decoration of the drug-loaded Pluronic micelles can enhance cellular uptake and tumor spheroids penetration, the cell apoptosis activity, and G_2/M phase cell cycle arrest of drug-loaded Pluronic micelles in KBv cells. Furthermore, c(RGDyK)-FP-DP displayed

stronger inhibition potency on the growth of KBv MDR tumor spheroids, as observed in the in vitro coculture cell-based model. Therefore, c(RGDyK)-decorated Pluronic micelles could be applied as a prospective dual-functional nanodrug delivery system for antiangiogenesis and drug resistance modulation.

Acknowledgments

This work was sponsored by National Natural Science Foundation of China (30901862), Postdoctoral Science Foundation of China (2014M550222), Shanghai Postdoctoral Sustentation Fund (14R21410500), National Basic Research Program of China (2013CB932500), and the Fundamental Research Funds for the Central Universities (22A201514055 ECUST). The authors also acknowledge the support from School of Pharmacy, Fudan University and the Open Project Program of Key Lab of

Smart Drug Delivery (Fudan University), Ministry of Education (SDD2014-2), and State Key Laboratory of Molecular Engineering of Polymers (Fudan University) (K2015-15).

Disclosure

The authors report no conflicts of interest in this work. The abstract of this paper (ID: 86827 for IJN) was presented at the Conference on Nanomedicine and NanoBiotechnology in the People's Republic of China from April 6 to 9, 2015 with the title "Dual-functional c(RGDyK)-decorated Pluronic micelles for antiangiogenesis and drug resistant tumor treatment in vitro" as a poster presentation with interim findings. The poster's abstract was published in "Poster Abstracts" in the journal of *Nanomedicine: Nanotechnology, Biology and Medicine* with the title "Dual-functional c(RGDyK)-decorated Pluronic micelles for antiangiogenesis and drug resistant tumor treatment in vitro". The actual paper, however, has never been published.

References

- Zhang B, Zhang Y, Liao Z, et al. UPA-sensitive ACP-PP-conjugated nanoparticles for multi-targeting therapy of brain glioma. *Biomaterials*. 2015;36:98–109.
- Ong BY, Ranganath SH, Lee LY, et al. Paclitaxel delivery from PLGA foams for controlled release in post-surgical chemotherapy against glioblastoma multiforme. *Biomaterials*. 2009;30(18):3189–3196.
- Lammers T, Hennink WE, Storm G. Tumour-targeted nanomedicines: principles and practice. *Br J Cancer*. 2008;99(3):392–397.
- Guo X, Shi C, Yang G, Wang J, Cai Z, Zhou S. Dual-responsive polymer micelles for target-cell-specific anticancer drug delivery. *Chem Mater*. 2014;26(15):4405–4418.
- Folkman J. What is the evidence that tumors are angiogenesis dependent? *J Natl Cancer Inst*. 1990;82(1):4–7.
- Bergers G, Benjamin LE. Tumorigenesis and the angiogenic switch. *Nat Rev Cancer*. 2003;3(6):401–410.
- Folkman J. Tumor angiogenesis: therapeutic implications. *N Engl J Med*. 1971;285:1182–1186.
- Carmeliet P, Jain RK. Angiogenesis in cancer and other diseases. *Nature*. 2000;407(6801):249–257.
- Cox D, Brennan M, Moran N. Integrins as therapeutic targets: lessons and opportunities. *Nat Rev Drug Discov*. 2010;9(10):804–820.
- Reynolds LE, Wyder L, Lively JC, et al. Enhanced pathological angiogenesis in mice lacking $\beta 3$ integrin or $\beta 3$ and $\beta 5$ integrins. *Nat Med*. 2002;8(1):27–34.
- Eliceiri BP, Cheresh DA. The role of αv integrins during angiogenesis: insights into potential mechanisms of action and clinical development. *J Clin Invest*. 1999;103(9):1227.
- Adulnirath A, Chung SW, Park J, et al. Cyclic RGDyK-conjugated LMWH-taurocholate derivative as a targeting angiogenesis inhibitor. *J Control Release*. 2012;164(1):8–16.
- De S, Razorenova O, McCabe NP, O'Toole T, Qin J, Byzova TV. VEGF-integrin interplay controls tumor growth and vascularization. *Proc Natl Acad Sci U S A*. 2005;102(21):7589–7594.
- Wang Z, Chui W-K, Ho PC. Integrin targeted drug and gene delivery. *Expert Opin Drug Deliv*. 2010;7(2):159–171.
- Eldar-Boock A, Miller K, Sanchis J, Lupu R, Vicent MJ, Satchi-Fainaro R. Integrin-assisted drug delivery of nano-scaled polymer therapeutics bearing paclitaxel. *Biomaterials*. 2011;32(15):3862–3874.
- Connelly JT, Garcia AJ, Levenston ME. Inhibition of in vitro chondrogenesis in RGD-modified three-dimensional alginate gels. *Biomaterials*. 2007;28(6):1071–1083.
- Gao Y, Chen L, Zhang Z, Chen Y, Li Y. Reversal of multidrug resistance by reduction-sensitive linear cationic click polymer/iMDR1-pDNA complex nanoparticles. *Biomaterials*. 2011;32(6):1738–1747.
- Takahashi S, Ito Y, Hatake K, Sugimoto Y. Gene therapy for breast cancer – review of clinical gene therapy trials for breast cancer and mdr1 gene therapy trial in cancer institute hospital. *Breast Cancer*. 2006;13(1):8–15.
- Clarke R, Leonessa F, Trock B. Multidrug resistance/p-glycoprotein and breast cancer: review and meta-analysis. *Semin Oncol*. 2005;32(6 Suppl 7):S9–S15.
- Mamot C, Drummond DC, Hong K, Kirpotin DB, Park JW. Liposome-based approaches to overcome anticancer drug resistance. *Drug Resist Updat*. 2003;6(5):271–279.
- Kabanov AV, Batrakova EV, Alakhov VY. Pluronic® block copolymers for overcoming drug resistance in cancer. *Adv Drug Deliv Rev*. 2002;54(5):759–779.
- Lee ES, Na K, Bae YH. Doxorubicin loaded pH-sensitive polymeric micelles for reversal of resistant MCF-7 tumor. *J Control Release*. 2005;103(2):405–418.
- Wang Y, Yu L, Han L, Sha X, Fang X. Difunctional Pluronic copolymer micelles for paclitaxel delivery: synergistic effect of folate-mediated targeting and Pluronic-mediated overcoming multidrug resistance in tumor cell lines. *Int J Pharm*. 2007;337(1–2):63–73.
- Wang Y, Li Y, Zhang L, Fang X. Pharmacokinetics and biodistribution of paclitaxel-loaded pluronic P105 polymeric micelles. *Arch Pharm Res*. 2008;31(4):530–538.
- Wang Y, Hao J, Li Y, et al. Poly(caprolactone)-modified Pluronic P105 micelles for reversal of paclitaxel-resistance in SKOV-3 tumors. *Biomaterials*. 2012;33(18):4741–4751.
- Chen L, Sha X, Jiang X, Chen Y, Ren Q, Fang X. Pluronic P105/F127 mixed micelles for the delivery of docetaxel against Taxol-resistant non-small cell lung cancer: optimization and in vitro, in vivo evaluation. *Int J Nanomedicine*. 2013;8:73.
- Chen Y, Zhang W, Gu J, et al. Enhanced antitumor efficacy by methotrexate conjugated Pluronic mixed micelles against KBv multidrug resistant cancer. *Int J Pharm*. 2013;452(1–2):421–433.
- Zhang W, Shi Y, Chen Y, Ye J, Sha X, Fang X. Multifunctional Pluronic P123/F127 mixed polymeric micelles loaded with paclitaxel for the treatment of multidrug resistant tumors. *Biomaterials*. 2011;32(11):2894–2906.
- Zhou Q, Zhang Z, Chen T, Guo X, Zhou S. Preparation and characterization of thermosensitive pluronic F127-b-poly(ϵ -caprolactone) mixed micelles. *Colloids Surf B: Biointerfaces*. 2011;86(1):45–57.
- Ahmed F, Pakunlu RI, Brannan A, Bates F, Minko T, Discher DE. Biodegradable polymersomes loaded with both paclitaxel and doxorubicin permeate and shrink tumors, inducing apoptosis in proportion to accumulated drug. *J Control Release*. 2006;116(2):150–158.
- Gustafson DL, Merz AL, Long ME. Pharmacokinetics of combined doxorubicin and paclitaxel in mice. *Cancer Lett*. 2005;220(2):161–169.
- Chen Y, Sha X, Zhang W, et al. Pluronic mixed micelles overcoming methotrexate multidrug resistance: in vitro and in vivo evaluation. *Int J Nanomedicine*. 2013;8:1463.
- Zhang W, Shi Y, Chen Y, et al. Enhanced antitumor efficacy by Paclitaxel-loaded Pluronic P123/F127 mixed micelles against non-small cell lung cancer based on passive tumor targeting and modulation of drug resistance. *Eur J Pharm Biopharm*. 2010;75(3):341–353.
- Gao H, Yang Z, Zhang S, Pang Z, Liu Q, Jiang X. Study and evaluation of mechanisms of dual targeting drug delivery system with tumor microenvironment assays compared with normal assays. *Acta Biomater*. 2014;10(2):858–867.
- Liu C, Liu F, Feng L, Li M, Zhang J, Zhang N. The targeted co-delivery of DNA and doxorubicin to tumor cells via multifunctional PEI-PEG based nanoparticles. *Biomaterials*. 2013;34(10):2547–2564.

36. Qiu L, Bae Y. Polymer Architecture and Drug Delivery. *Pharm Res.* 2006;23(1):1–30.
37. Wang H, Zhao Y, Wu Y, et al. Enhanced anti-tumor efficacy by co-delivery of doxorubicin and paclitaxel with amphiphilic methoxy PEG-PLGA copolymer nanoparticles. *Biomaterials.* 2011;32(32):8281–8290.
38. Rapoport N, Pitt WG, Sun H, Nelson JL. Drug delivery in polymeric micelles: from in vitro to in vivo. *J Control Release.* 2003;91(1–2):85–95.
39. Polisenio L, Tuccoli A, Mariani L, et al. MicroRNAs modulate the angiogenic properties of HUVECs. *Blood.* 2006;108(9):3068–3071.
40. Matsui J, Wakabayashi T, Asada M, Yoshimatsu K, Okada M. Stem cell factor/c-kit signaling promotes the survival, migration, and capillary tube formation of human umbilical vein endothelial cells. *J Biol Chem.* 2004;279(18):18600–18607.
41. Batrakova EV, Kabanov AV. Pluronic block copolymers: evolution of drug delivery concept from inert nanocarriers to biological response modifiers. *J Control Release.* 2008;130(2):98–106.
42. Desgrosellier JS, Cheresh DA. Integrins in cancer: biological implications and therapeutic opportunities. *Nat Rev Cancer.* 2010;10(1):9–22.
43. Lee S, Kim J, Shim G, et al. Tetraiodothyroacetic acid-tagged liposomes for enhanced delivery of anticancer drug to tumor tissue via integrin receptor. *J Control Release.* 2012;164(2):213–220.
44. AbuHammad S, Zihlif M. Gene expression alterations in doxorubicin resistant MCF7 breast cancer cell line. *Genomics.* 2013;101(4):213–220.
45. de Hoon JPJ, Veeck J, Vriens BEPJ, Calon TGA, van Engeland M, Tjan-Heijnen VCG. Taxane resistance in breast cancer: a closed HER2 circuit? *Biochim Biophys Acta.* 2012;1825(2):197–206.
46. Minchinton AI, Tannock IF. Drug penetration in solid tumours. *Nat Rev Cancer.* 2006;6(8):583–592.
47. Dhanikula RS, Argaw A, Bouchard J-F, Hildgen P. Methotrexate loaded polyether-copolyester dendrimers for the treatment of gliomas: enhanced efficacy and intratumoral transport capability. *Mol Pharm.* 2008;5(1):105–116.
48. Davies C, Müller H, Hagen I, Gärseth M, Hjelstuen M. Comparison of extracellular matrix in human osteosarcomas and melanomas growing as xenografts, multicellular spheroids, and monolayer cultures. *Anticancer Res.* 1996;17(6D):4317–4326.
49. Jiang X, Sha X, Xin H, et al. Integrin-facilitated transcytosis for enhanced penetration of advanced gliomas by poly(trimethylene carbonate)-based nanoparticles encapsulating paclitaxel. *Biomaterials.* 2013;34(12):2969–2979.
50. Schechner JS, Nath AK, Zheng L, et al. In vivo formation of complex microvessels lined by human endothelial cells in an immunodeficient mouse. *Proc Natl Acad Sci U S A.* 2000;97(16):9191–9196.

Supplementary material

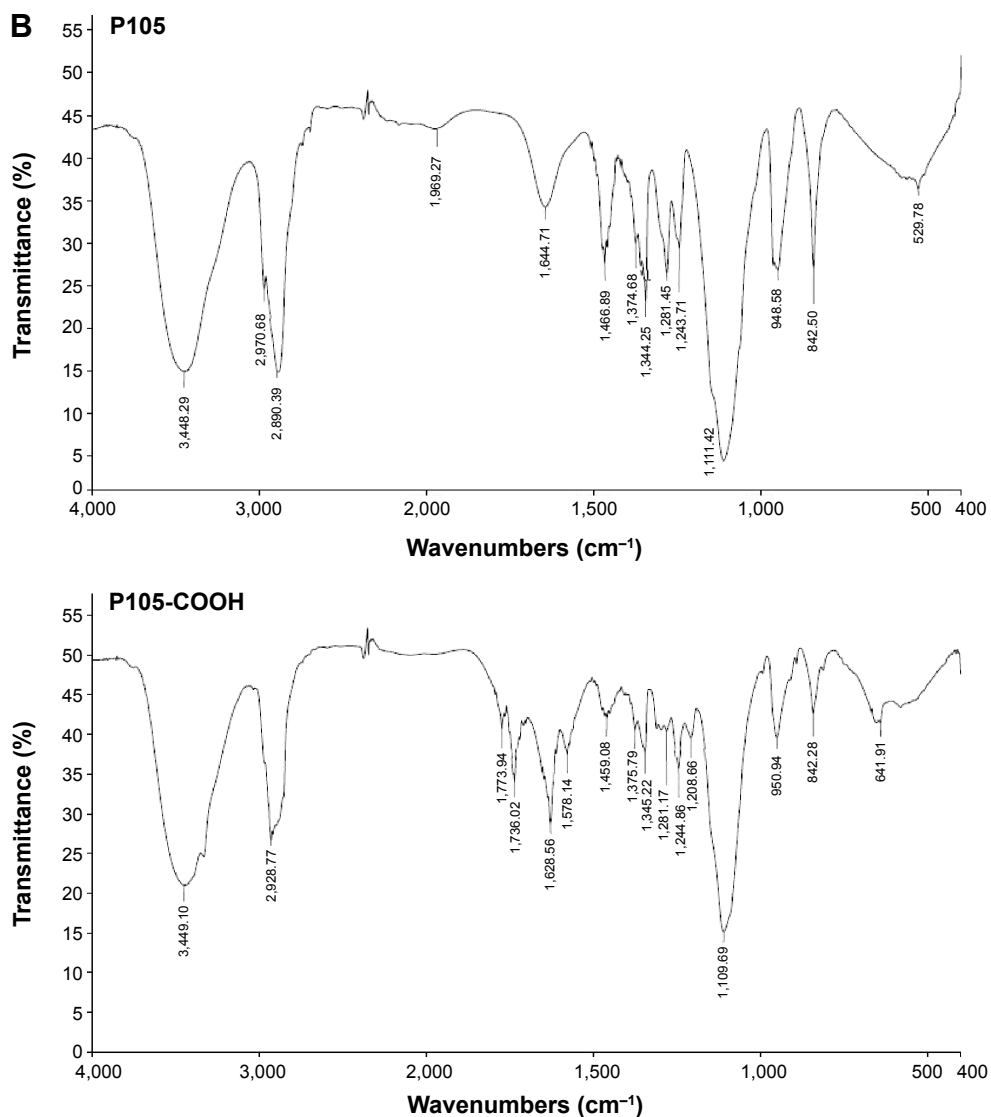
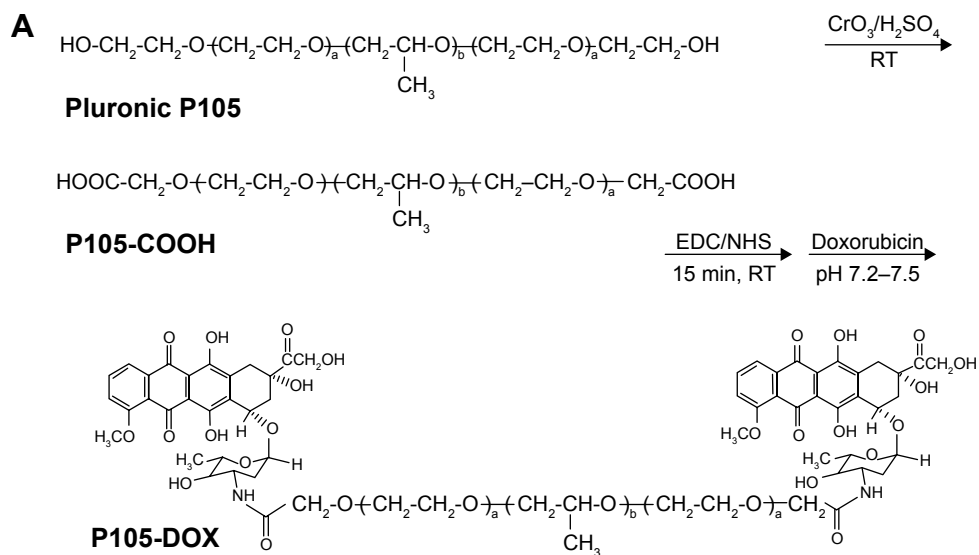


Figure S1 (Continued)

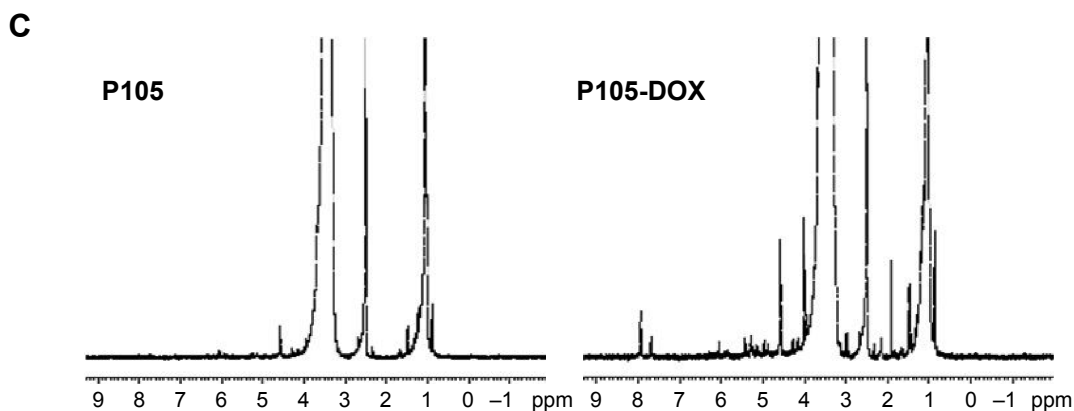


Figure S1 The synthetic route and characterization of P105-DOX.

Notes: Synthetic route of P105-DOX conjugate ($a=36$, $b=56$) (**A**); FT-IR spectra of Pluronic P105 and P105-COOH (**B**); $^1\text{H-NMR}$ spectra of P105 and P105-DOX in DMSO-d_6 (**C**).

Abbreviations: DOX, doxorubicin; FT-IR, Fourier transform infrared spectroscopy; DMSO, dimethyl sulfoxide; $^1\text{H-NMR}$, $^1\text{H-nuclear magnetic resonance spectroscopy}$; RT, room temperature; EDC, 1-ethyl-3-(3-dimethylaminopropyl)-carbodiimide; NHS, *N*-hydroxysuccinimide.

International Journal of Nanomedicine

Publish your work in this journal

The International Journal of Nanomedicine is an international, peer-reviewed journal focusing on the application of nanotechnology in diagnostics, therapeutics, and drug delivery systems throughout the biomedical field. This journal is indexed on PubMed Central, MedLine, CAS, SciSearch®, Current Contents®/Clinical Medicine,

Submit your manuscript here: <http://www.dovepress.com/international-journal-of-nanomedicine-journal>

Journal Citation Reports/Science Edition, EMBase, Scopus and the Elsevier Bibliographic databases. The manuscript management system is completely online and includes a very quick and fair peer-review system, which is all easy to use. Visit <http://www.dovepress.com/testimonials.php> to read real quotes from published authors.

Dovepress